Journal of Engineering Physics and Thermophysics, Vol. 66, No. 1, 1994

FLOW AND HEAT TRANSFER CHARACTERISTICS IN THE CHANNELS OF PLATE-TYPE HEAT EXCHANGERS WITH CORRUGATED PLATES*

L. P. Pertsev and L. M. Ul'ev

UDC 66.045.3

Fluid flow in the channels of plate-type heat exchangers is modeled by a two-dimensional flow in plane channels with distributed resistance to fluid flow determined by the nature of the corrugation of the plates. Such an approach permits one to find the distribution of pressure and fluid flow velocity over the plate field, and then, with the use of the semiempirical dependence of heat transfer coefficient on pressure gradient, to determine the distribution and mean value of the heat transfer coefficient on the field of the heat exchanger plate.

The most important problem with respect to increasing the national income in industry is a reduction in the metal content and energy consumption of articles, as well as bringing new energy-saving production processes to a commercial level. In the field of heat exchanging equipment the problem amounts to a further decrease in of the overall size and specific metal content of appraratus per unit of thermal performance.

To solve the above problem, it is necessary to find new, more efficient engineering solutions and embody them in the designs of plate-type heat exchangers. This is the aim of the present study.

The price of one industrial plate heat exchanger runs into several tens of millions of rubles, and therefore it would be too costly to carry out experiments on such apparatus for determining efficient heat transfer surfaces; this being so, interest has recently increased in the development of scientifically justified methods of investigation and calculation of the elements of heat-exchanging equipment.

The construction and investigation of a model of convective heat transfer in the channels of screen-flow-type heat exchangers composed of corrugated plates (Fig. 1) involve great difficulties because of the complex spatial motion of fluid. The solution of the differential equations of transfer for turbulent flow, most interesting from the practical standpoint, is not always possible, even for straight channels [1]. Therefore, in practice the pressure drop for the flow of fluid with constant properties in the channel of a heat exchanger is usually determined by the Darcy-Weisbach formula

$$\Delta P = \xi \frac{L}{d_{\text{eq}}} \frac{\rho \bar{V}^2}{2}. \tag{1}$$

An expression for ξ in flow through channels of plate-type heat exchangers was obtained in [3-5]

$$\xi = \frac{0.34 \exp(1.51 \tan\varphi)}{\text{Re}^{0.25-0.06\tan\varphi}} [1.24 \exp(-0.37 \tan\varphi)^{\beta}], \tag{2}$$

where β is a parameter determined by the geometric dimensions of a crimp, its height h, and by the spacing between the crests of neighboring crimps l.

* The paper was submitted to the 2nd Minsk International Heat and Mass Transfer Forum held from the 18th to the 22nd of May, 1992 (see J. Eng. Phys., Vol. 62, No. 6, 1993).

Ukrainian Scientific-Research and Design Institute of Chemical Engineering, Khar'kov. Translated from Inzhenerno-Fizicheskii Zhurnal, Vol. 66, No. 1, pp. 3-15, January, 1994. Original article submitted May 18, 1992.

1062-0125/94/6601-0001$12.50

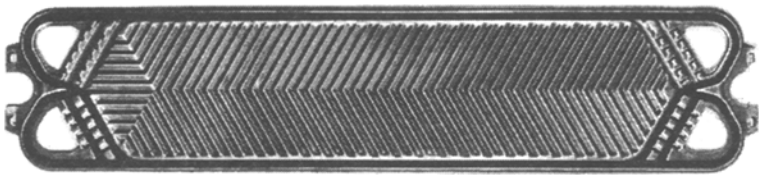

Fig. 1. The plate of a commercially produced heat exchanger of type 0.3E.

Relation (1) is also valid for flow in porous media [6]; moreover, thanks to the cellular structure of the channel, the flow between corrugated plates can be considered as two-dimensional in a porous medium located between smooth and parallel plates, i.e., as a nonlinear analog of the Hele-Shaw cell in the form of a plate heat exchanger [7, 8].

Relation (1) can be rewritten in the form

$$\frac{dP}{dL} = -kf(\bar{V}), \tag{3}$$

where k depends only on the geometric dimensions of the channel, and $f(\mathrm{V})$ is usually a power function of velocity [2].

To determine the pressure gradient for two-dimensional motion in a porous medium we may write

$$\operatorname{grad} P = -k_{ij} f_j(\mathbf{V}). \tag{4}$$

Here k_{ij} is the tensor quantity which characterizes the resistance of the medium; physically it is similar to the reciprocal of the permeability tensor in the theory of filtration; V is the seepage velocity of the fluid.

From Fig. 1 and relation (2) it is seen that in the heat exchanger channel there are two distinct, mutually perpendicular directions which are extremal for the resistance coefficients. Therefore the medium in which fluid flows can be regarded as being orthotropic.

Introducing a coordinate system with the directions of axes along the principal axes of the tensor k_{ij} (Fig. 2), we rewrite relation (4) in the form

$$\operatorname{grad} P = -\mathbf{i}k_x \operatorname{sign}(V_x) |V_x|^{s_x} - \mathbf{j}k_y \operatorname{sign}(V_y) |V_y|^{s_y}, \tag{5}$$

where s_x, $s_y = s(\beta, x, y)$; k_x, k_y are the resistance coefficients along and across the channel.

Using the dimensionless variables and parameters

$$\Pi = \frac{Pd_{eq}^2\rho}{\mu^2}, \quad Rv_x = \frac{d_{eq}V_x\rho}{\mu}, \quad Rv_y = \frac{d_{eq}V_y\rho}{\mu}, \quad \Lambda = \frac{d_{eq}}{L}, \quad \chi = \frac{x}{L}, \quad \eta = \frac{y}{L},$$

we can rewrite projections (5) onto the coordinate axes and the continuity equation in the form

$$\Lambda \frac{\partial \Pi}{\partial \chi} = -\kappa_x \operatorname{sign}(Rv_x) |Rv_x|^{s_x}, \tag{6}$$

$$\Lambda \frac{\partial \Pi}{\partial \eta} = -\kappa_y \operatorname{sign}(Rv_y) |Rv_y|^{s_y}, \tag{7}$$

$$\frac{\partial Rv_x}{\partial \chi} + \frac{\partial Rv_y}{\partial \eta} = 0. \tag{8}$$

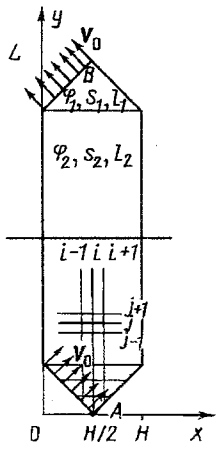

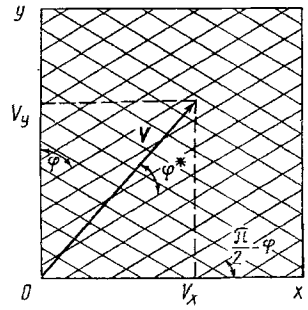

Fig. 2. Computational scheme.

Fig. 3. Determination of the angle between the seepage velocity and crimps.

The boundary conditions for this system of equations are the conditions of impermeability on the side walls of the channel and constant pressure gradients at the inlet and exit of it prescribed by the constant flow rate of fluid (Fig. 2):

$$\left(\frac{1}{\kappa_x}\frac{\partial \Pi}{\partial \chi}\right)^{2/s_x} + \left(\frac{1}{\kappa_y}\frac{\partial \Pi}{\partial \eta}\right)^{2/s_y} = \mathrm{Re}_0^2, \quad \begin{cases} 0 \le \eta \le \eta_1; \\ \eta_2 \le \eta \le \eta_0; \end{cases} \quad 0 \le \chi \le \frac{\chi_0}{2}, \tag{9}$$

$$\left(\frac{1}{\kappa_x}\frac{\partial \Pi}{\partial \chi}\right)^{2/s_x} + \left(\frac{1}{\kappa_y}\frac{\partial \Pi}{\partial \eta}\right)^{2/s_y} = 0, \quad \begin{cases} 0 \le \eta \le \eta_1; \\ \eta_2 \le \eta \le \eta_0; \end{cases} \quad \frac{\chi_0}{2} \le \chi \le \chi_0, \tag{10}$$

$$\frac{\partial \Pi}{\partial \chi} = 0, \quad \eta_1 \le \eta \le \eta_2, \quad \begin{cases} \chi = 0; \\ \chi = \chi_0, \end{cases} \tag{11}$$

where $\eta_1 = y_1/L$; $\eta_2 = y_2/L$; $\eta_0 = 1$; $\lambda_0 = H/L$.

These conditions are written for the "left-hand" channel. They have a similar form also for the "right-hand" channel.

Differentiating Eqs. (6) and (7) with respect to the corresponding coordinate, we obtain velocity derivatives whose substitution into the continuity equation yields an expression which describes the pressure field in the heat-exchanger channel

$$\kappa_y s_y R v_y^{s_y - 1} \frac{\partial^2 \Pi}{\partial \chi^2} + \kappa_x s_x R v_x^{s_x - 1} \frac{\partial^2 \Pi}{\partial \eta^2} = 0, \tag{12}$$

$$R v_x = -\operatorname{sign}\left(\frac{\partial \Pi}{\partial \chi}\right) \kappa_x^{-1/s_x} \left(\Lambda \left| \frac{\partial \Pi}{\partial \chi} \right|\right)^{1/s_x}, \tag{13}$$

$$R v_y = -\operatorname{sign}\left(\frac{\partial \Pi}{\partial \eta}\right) \kappa_y^{-1/s_y} \left(\Lambda \left| \frac{\partial \Pi}{\partial \eta} \right|\right)^{1/s_y}. \tag{14}$$

The system of equations (9)-(14) can be integrated numerically by the time-dependent technique. For this purpose, Eq. (12) is formulated in a nonstationary form, i.e., its left-hand side is equated with the derivative $\partial \Pi/\partial \tau$, where

τ is some dimensionless time. The spatial derivatives in Eqs. (12)-(14) are approximated by central differences on a computational grid (Fig. 2). Thus, a system of ordinary differential equations is obtained that describes the pressures $\Pi_{i,j}$ at each point of the division (i, j), which are subsequently integrated by the Gear method up to complete development of a steady state. In doing so, we ensure agreement with the condition of constant flow rate in each cross section on the grid.

As a result of integration we obtain the distribution of the dimensionless pressure and velocity components over the field of the heat exchanger plate.

Using these data and the semiempirical dependence of the heat transfer coefficient on the resistance coefficient [9]

$$\alpha = \frac{0.14\,\lambda\,\mathrm{Re}\,\mathrm{Pr}\sqrt{\xi}}{d_{\mathrm{eq}}\left\{\ln\left(\mathrm{Re}\sqrt{\xi}/760\right) + 2\left[\mathrm{Pr} + \ln\left(1 + 5\,\mathrm{Pr}\right)\right]/\sqrt{\vartheta}\right\}}, \tag{15}$$

(where ϑ is the pressure gradient function, Pr is the Prandtl number) we obtain the distribution of the local coefficients over the field of the plate. But first we must determine ξ for any direction of the seepage velocity in the channel between the plates (Fig. 3).

Relation (2) was obtained on the condition that V is directed along the plate and that in such a case φ is the angle of inclination of the crimps to the velocity direction. From Fig. 3 it is seen that when the velocity changes direction by $\pi/2$, the angle of inclination of the crimps to the flow velocity undergoes a change by $\pi/2-\varphi$. This makes it possible to determine the angle of inclination of the crimps to the fluid flow φ^* at the known components V_x and V_y, i.e., ξ in Eq. (15) will be determined for the angle

$$\varphi^* = \varphi + \left(1 - \frac{4\varphi}{\pi}\right)\left|\arctan\left(\frac{V_x}{V_y}\right)\right|. \tag{16}$$

Under identical conditions for heat carriers, the velocity distribution in adjacent channels is symmetric about the principal axis of the plate, i.e., the heat transfer coefficients will also be symmetrical

$$|V'_{i,j}| = |V''_{N+1-i,j}| \rightarrow \alpha'_{i,j} = \alpha''_{N+1-i,j}, \tag{17}$$

where ' is for the "left-hand" channel and '' is for the "right-hand" channel, $i = 1, 2, \ldots, N$, $j = 1, 2, \ldots, M$.

In this case the heat conduction coefficients are defined as

$$K_{i,j} = \left(\frac{1}{\alpha_{i,j}} + \frac{\delta_{\mathrm{pl}}}{\lambda_{\mathrm{pl}}} + \frac{1}{\alpha_{N+1-i,j}}\right)^{-1}, \tag{18}$$

where $\delta_{\mathrm{pl}} = 10^{-3}$ m and $\lambda_{\mathrm{pl}} = 60$ W/(m·K) are the thickness and the thermal conductivity of the plate, respectively.

The adequacy of the model was checked by comparing the calculated and experimental data obtained on standard heat exchangers with plates of type 0.6 [2, 10]: $\varphi = 60^{\circ}$ over the entire field, $L = 1.1$ m, $H = 0.55$ m, $l =$ 18 mm, $h = 4$ mm. Experiments were carried out for a fluid with the parameters $c = 4.174$ kJ/(kg·K), $\mu = 0.4997 \cdot 10^{-3}$ Pa·sec, $\lambda_{\mathrm{fl}} = 0.648$ W(m·K). Comparison shows that the mean relative errors in the determination of the pressure difference and mean heat conduction coefficient do not exceed 15% (Fig. 4).

Similar investigations were carried out for typical heat exchangers with plates of type R 0.6-2 [10] where the inclination angle of crimps on distributing portions can be regarded equal to $\varphi_1 = 15^{\circ}$ and over the main field to $\varphi = 40^{\circ}$ (see Fig. 2). In this case, on the interfaces between the zones with different values of φ the following conjugation conditions should be fulfilled:

$$\frac{1}{\kappa_{y1}\,\Delta\eta_1}\left(\frac{\partial\Pi}{\partial\eta}\right)_1 = \frac{1}{\kappa_{y2}\,\Delta\eta_2}\left(\frac{\partial\Pi}{\partial\eta}\right)_2, \tag{19}$$

where $\Delta\eta_1$ and $\Delta\eta_2$ are the steps of the grid over η in zones 1 and 2 (Fig. 2).

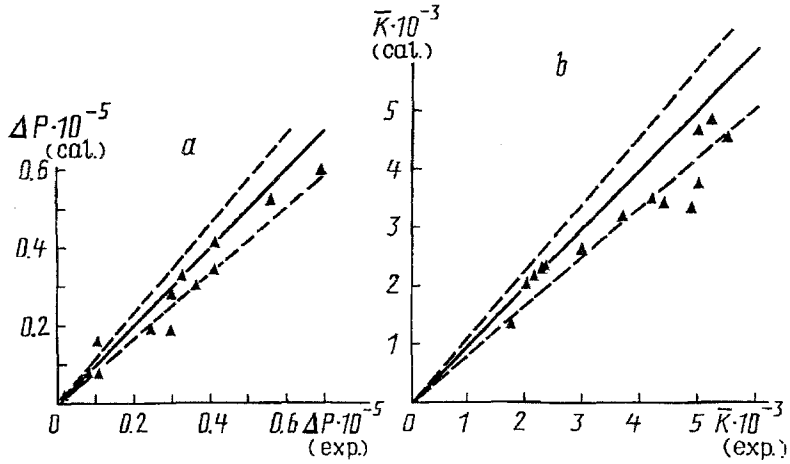

Fig. 4. Comparison of the calculated values of pressure drop (a) and mean heat conduction coefficient (b) with experimental results (points); solid line; perfect coincidence; dashed line, boundaries of the 15% deviation zone ΔP, Pa; $\bar{K}$, W/(m^2·K).

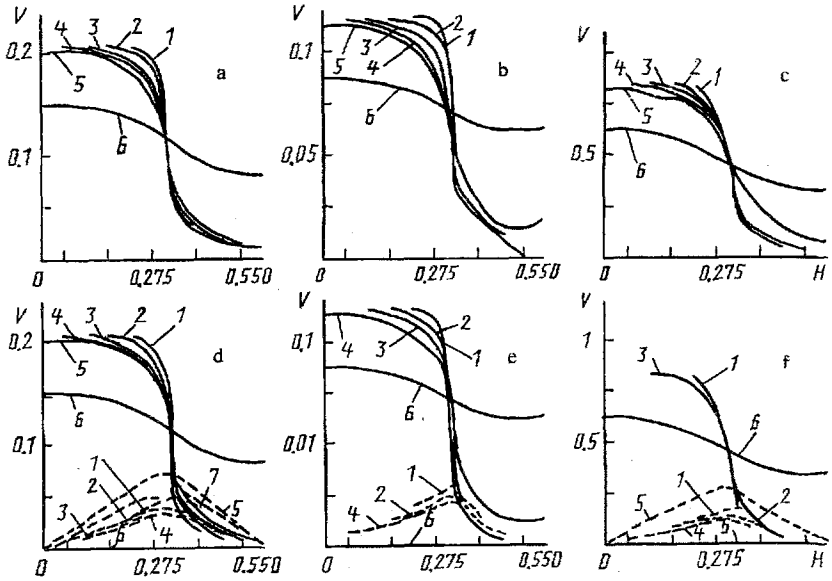

Fig. 5. Distribution of the velocity modulus (a, b, c) and of the components of V_y (solid lines), V_x (dashed lines) (d, e, f) of the heat exchanger R 0.6-2 across the channel: a, d) $Q = 0.278 \cdot 10^{-3}$ m^3/sec; b, e) $0.167 \cdot 10^{-3}$; c, f) $0.956 \cdot 10^{-3}$; distance from the start of the plate: 1) 4 cm; 2) 8; 3) 12; 4) 16; 5) 20; 6) 55; 7) 28 cm. V, m/sec; H, m.

Due to the fact that the resistance of corrugation to the fluid flow along the plate is much smaller than the resistance accross the plate ($\kappa_{x1}/\kappa_{y1} \approx 80$, $\kappa_{x2}/\kappa_{y2} \approx 6$), the fluid has no time to be distributed uniformly over the cross section of the channel, and the fluid velocity from the side of the collectors turns out to be higher for any cross section (Fig. 5). Due to such a distribution of the velocity, the distribution of the heat conduction coefficients is very nonuniform over the plate width (Fig. 6), and this leads to elongated peak-like distributions of heat conduction coefficients across the plate.

On the distributing portions of flow, the velocity modulus is somewhat higher than on the main field, since the cross section there is smaller. But the value of V_x is larger, i.e., distribution of fluid flow across the channel takes place. Then V_x decreases to 0, and the flow becomes virtually rectilinear (Fig. 5). Owing to such a distribution of velocity, the heat transfer and heat conduction coefficients on distributing portions are higher than on the main

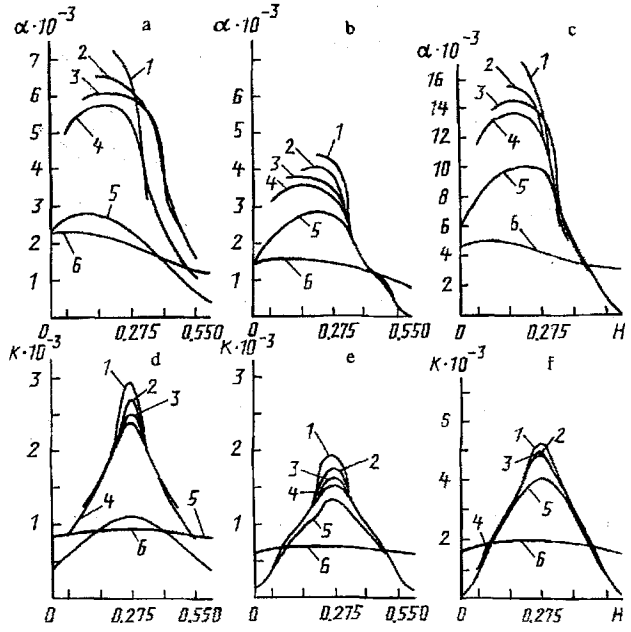

Fig. 6. Distribution of the heat transfer coefficient α and heat conduction coefficient K across the channel. Designations are the same as those in Fig. 5. α, W/(m^2·K).

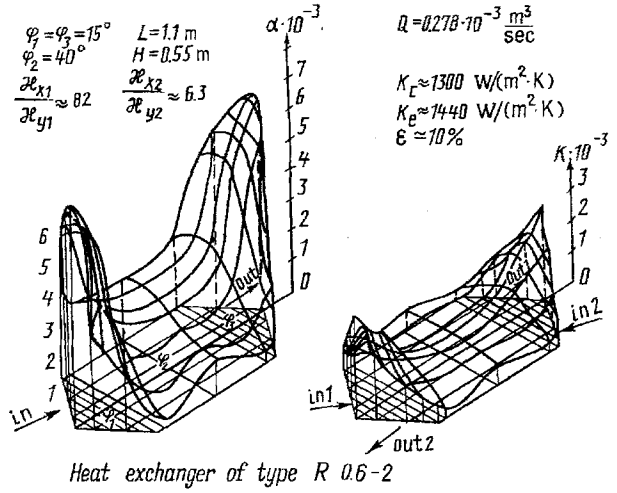

Fig. 7. Distribution of the heat transfer coefficient α and heat conduction coefficient K for the plate R 0.6-2 ($\overline{K}$, calculated value; K, experimental value).

field (Fig. 7), with the distribution of K being symmetric with respect to the principal axis of the plate due to the symmetric distribution of α in adjacent channels.

The results show that in R 0.6-2 heat exchangers the corrugation of plates is not good, at least on the distributing portions.

The effect of changes in the corrugated field of plates on heat transfer was investigated numerically for 0.6-type plates and their modifications.

Let us consider heat transfer at flow rates in adjacent channels $Q = 0.137 \cdot 10^{-2}$ m^3/sec for five versions of the corrugated field: a) $\varphi_1 = \varphi_2 = 60^\circ$, $l_1 = l_2 = 18$ mm, $h_1 = h_2 = 4$ mm; b) $\varphi_1 = 60^\circ$, $\varphi_2 = 70^\circ$, $l_1 = l_2 = 18$ mm, $h_1 = h_2 = 4$ mm; c) $\varphi_1 = 70^\circ$, $\varphi_2 = 65^\circ$, $l_1 = 36$, $l_2 = 18$ mm; $h_1 = h_2 = 4$ mm; d) $\varphi_1 = \varphi_2 = 60^\circ$, $l_1 = l_2 = 18$ mm, $h_1 = h_2 = 3$ mm; e) $\varphi_1 = 70^\circ$, $\varphi_2 = 65^\circ$, $l_1 = 36$, $l_2 = 18$ mm, $h_1 = h_2 = 3$ mm.

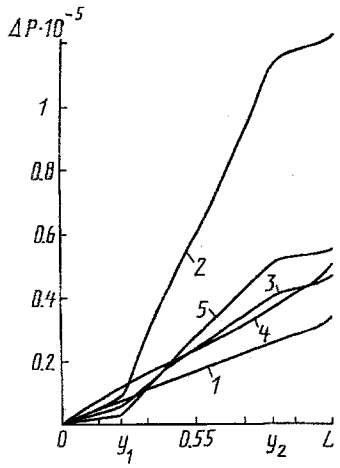

Fig. 8. Distribution of pressure along the heat exchanger channel: 1) for version a); 2) for b); 3) for c); 4) for d); 5) for e). L, m.

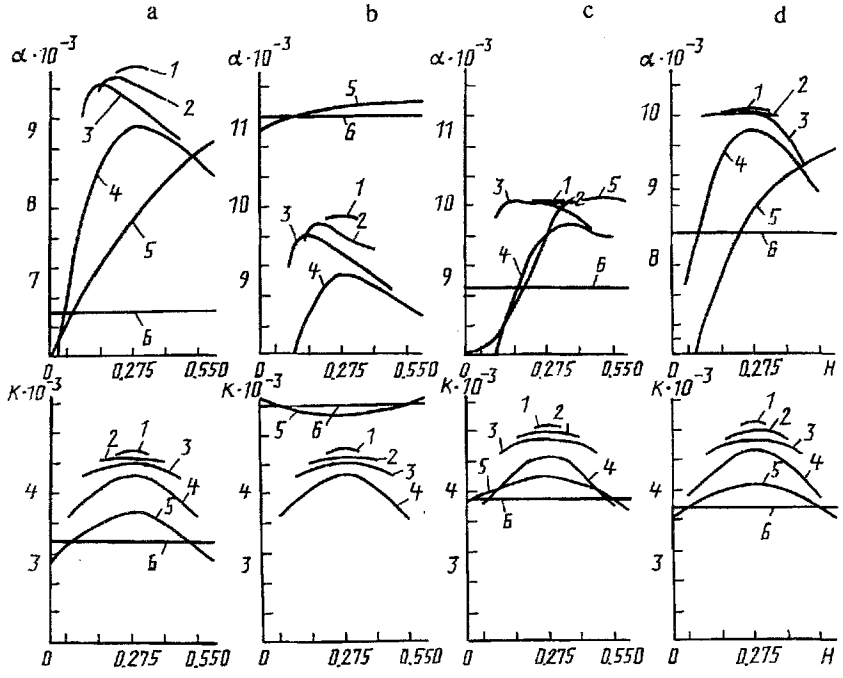

Fig. 9. Distribution of the heat transfer and heat conduction coefficients across the channel for versions a), b), c), and d) (a-d, respectively); distance along the axis y from the start of the plate: 1) 4 cm; 2) 8; 3) 12; 4) 16; 5) 24; 6) 55 cm.

The pressure distribution along the channel is determined by the nature of corrugation of the plates. In cases (a) and (d) it is almost linear, since the corrugation of the plates is homogeneous.

In other cases, at the boundaries of the distributing portions the inclination angle of crimps, as well as the resistance to flow and grad P, change jumpwise (Fig. 8).

A similar distribution is also observed for the heat transfer coefficients on the field of the plate. In places where the value of grad P is high, they are maximal (Fig. 9). On the distributing portions the profile of α is asymmetrical since the velocity profile has not formed as yet. This is more pronounced for versions (a) and (d) (Figs. 9 and 10). In case (a), $\kappa_{y2} > \kappa_{y1}$, whereas $\kappa_{y1}/\kappa_{x1} \approx 0.1$ and $\kappa_{y2}/\kappa_{x2} \approx 0.01$. This promotes a more uniform distribution of fluid over the channel cross section. Therefore, α and K at the inlet and exit are distributed more uniformly, whereas on the main field their values are higher than on the distributing portions (Fig. 11).

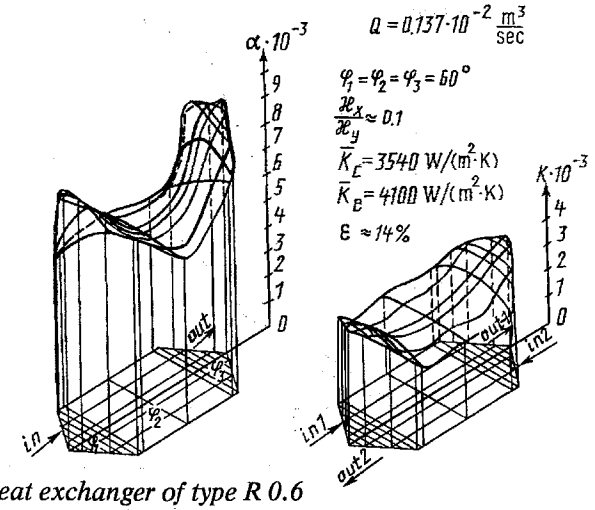

Heat exchanger of type R 0.6

Fig. 10. Distribution of the heat transfer coefficient α and heat conduction coefficient K over the field of the plate for version a).

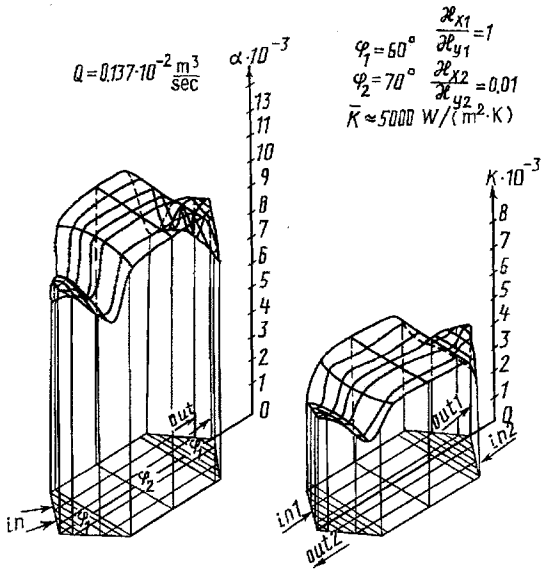

Fig. 11. Distribution of the heat transfer coefficient α and heat conduction coefficient K over the field of the plate for version b).

The mean heat conduction coefficient $\overline{K}$ for version (b) is 41.2% higher than for the initial version (a). But here ΔP increases by 243%. In case (b) $\overline{K}$ grows by 24.3% as compared with (a) and ΔP grows by 40%. In cases (d) and (e) $\overline{K}$ increases by a smaller value than the mean relative error, while ΔP grows appreciably, and one can say that the change in the corrugated field is most advantageous for version (c).

For thermal treatment of high-viscosity fluids with a strong temperature dependence of their rheological properties, a plate with curvilinear S-like crimps was developed [11-13] (Fig. 12). To determine the efficiency of these plates in treating fluids with constant properties, a number of numerical and full-scale experiments were carried out for such fluids.

Investigations were carried out with plates 0.3E: $L = 1.1$ m; $H = 0.25$ m; $h = 4$ mm; $R = 0.7$ m; the spacing between the adjacent crests along the central axis was $l_0 = 20$ mm for the following versions of corrugation: (1) a plate of "crow's feet"-type with $\varphi = 60^\circ$; (2) a plate with S-like crimps and a constant angle of inclination along the central axis $\varphi_0 = 60^\circ$; (3) S-crimps with the change in the inclination angle along the central axis from 45 to 70°; (4) S-crimps with the change in φ_0 from 45 to 75°; 5) S-crimps with φ_0 changing from 50 to 70°. The fluid properties

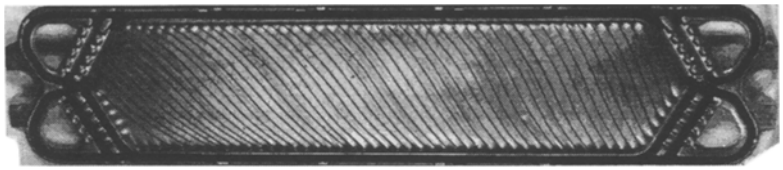

Fig. 12. Experimental plate with S-like crimps.

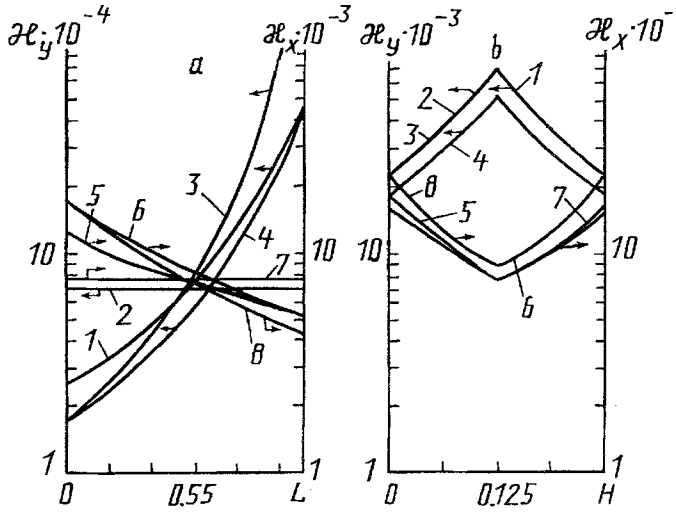

Fig. 13. Distribution of the resistance coefficient: a) along the central axis of the channel; b) across the channel at $y = L/2$; 1, 2, 3, 4) distribution of κ_y; 5, 6, 7, 8) κ_x; 1, 5) for S-like crimps with inclination angle along the axis equal to 50-70°; 2, 7) S-like crimps with inclination angle along the axis equal to 60°; 3, 8) 45-75°; 4, 6) 45-70°. L, m.

remained as before, whereas the flow rate was equal to $Q = 5 \cdot 10^{-4}$ m^3/sec. The distribution of κ_x and κ_y for the versions selected is shown in Fig. 13.

Since κ_x and κ_y in channels with S-like corrugation of plates are functions of the coordinates, Eq. (12) assumes the form

$$\kappa_y s_y Rv_y^{s_y-1}\left(\Lambda\frac{\partial^2\Pi}{\partial\chi^2}+Rv_x^{s_x}\frac{\partial\kappa_x}{\partial\chi}\right)+\kappa_x s_x Rv_x^{s_x-1}\left(\Lambda\frac{\partial^2\Pi}{\partial\eta^2}+Rv_y^{s_y}\frac{\partial\kappa_y}{\partial\eta}\right)=0, \qquad (12')$$

where it is taken into account that the coefficients κ depend on φ more strongly than the exponents s. The boundary conditions remained as before, as well as the solution technique.

In case (1) the resistance to fluid flow along the channel is somewhat higher than that across the channel, while the length of the channel is large as compared with its width. This promotes the establishment of a uniform velocity profile (Fig. 14).

In channels with plates of version (2) the distribution of κ_x and κ_y across the channel is nonuniform: κ_y is maximum at the center and decreases toward the periphery of the channel; κ_x, conversely. This means that around the periphery the resistance to fluid motion along the channel will be smaller while the fluid flow will be larger (Fig. 14). In view of this, the transverse velocity component V_x over the distributing portion is somewhat higher in the second case than in the first, and a greater portion of fluid is directed here to the side walls.

While in cases (1) and (2) the distribution of velocities on the plate is symmetric about the middle line, there is no such symmetry for versions (3) and (4). At the inlet, in the case of small inclination angles of crimps, $\kappa_x >> \kappa_y$, and as a result the fluid has no time to be distributed uniformly over the width of the inlet section; therefore V_y is higher near the collector hole within the distributing portion (Fig. 15). Hereafter the fluid velocity

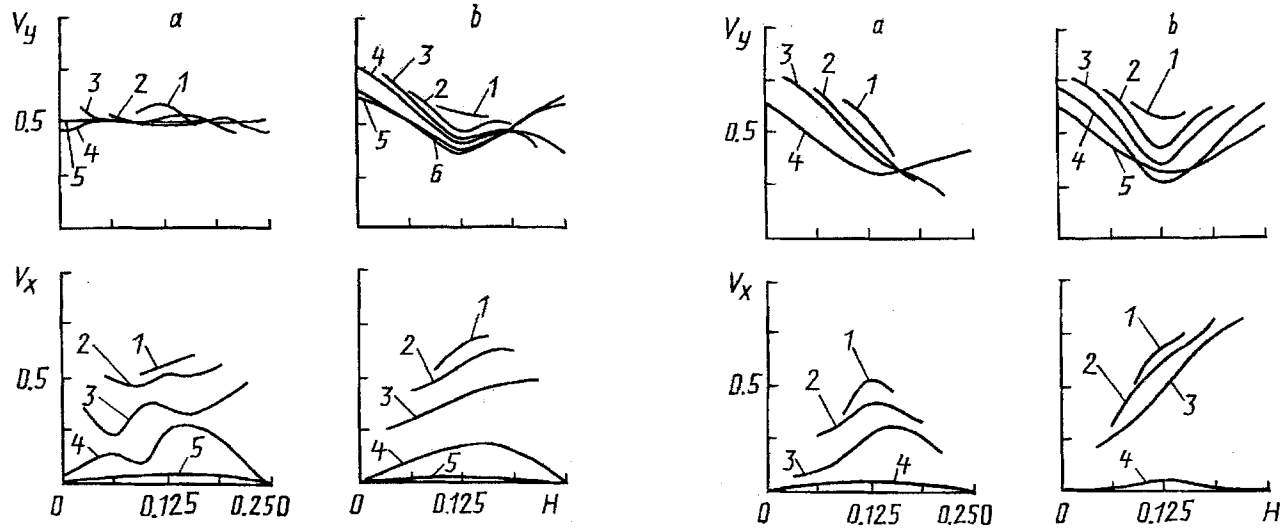

Fig. 14. Distribution of fluid velocity components across the channel: a) for a plate of crow's feet type; b) for a plate with S-like crimps $\varphi_0 = 60^\circ$; 1) y = 0.025 m; 2) 0.05; 3) 0.075; 4) 0.1; 5) 0.19; 6) 0.55 m.

Fig. 15. Distribution of the fluid velocity components across the channel for S-like plates with inclination angles of crimps equal to 45-70°; a) first half of the plate; 1) y = 0.025 m; 2) 0.05; 3)0.075; 4) 0.1 m; b) second half of the plate; 1) L-y = 0.025 m; 2) 0.05; 3) 0.075; 4) 0.1; 5) 0.55 m.

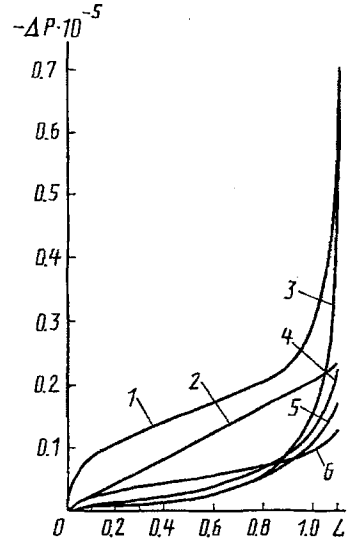

Fig. 16. Distribution of pressure drop along the central axis of the channel: 1) for a plate with S-like crimps and φ = 70-75°; 2) "crow's feet"; 3) φ = 45-75°; 4) 50-70°; 5) 45-70°.

distribution in the channel is similar to that in the 2nd case, as the resistance to motion at the periphery is smaller than at the center. However, at the exit, due to the fact that $\kappa_y >> \kappa_x$ (large inclination angles), the transverse velocity component increases (Fig. 15).

The pressure distribution at constant flow rate is determined in the main by the character of distribution of the resistance coefficients. In the case of uniform distribution, the pressure drop along the channel is almost linear (Fig. 16). In case (2) the pressure gradient is smaller than in (1), since the resistance to motion around the periphery of the channel is smaller. For versions (3), (4), and (5) ΔP is much smaller than in the former two versions, since here the inclination angles of crimps toward the axis is smaller, i.e., κ_y is also smaller. But with

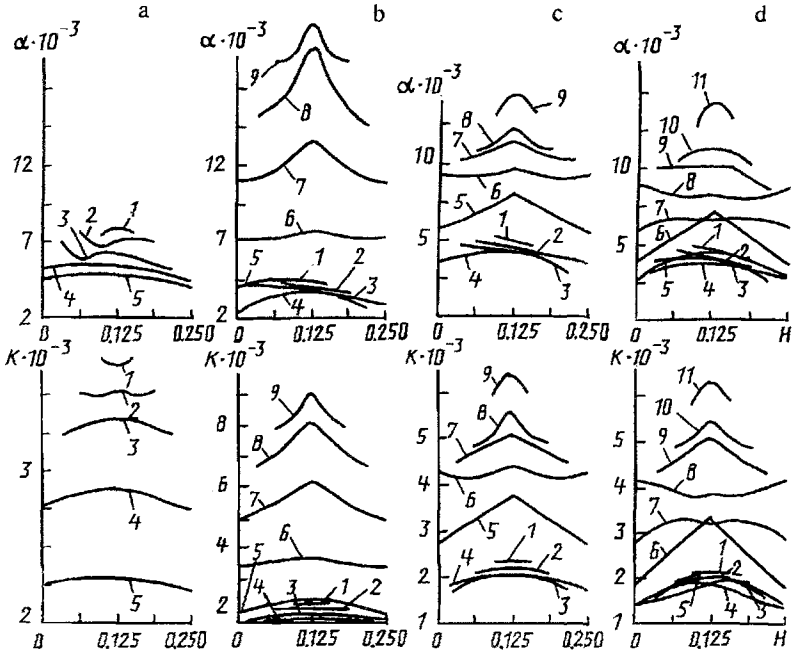

Fig. 17. Distribution of the coefficients of heat transfer α and heat conduction K across the channel: a) for version 1: 1) $y = 0.025$ m; 2) 0.05; 3) 0.75; 4) 0.1; 5.).55 m; b, c) for versions 4 and 5: 1) $y = 0.025$ m; 2) 0.05; 3) 0.075; 4) 0.1; 5) 0.19; 6) 0.55; 7) 1.025; 8) 1.05; 9) 1.075 m; d) for version 3: 1) $y = 0.025$ m; 2) 0.05; 3) 0.075; 4) 0.1; 5) 0.19; 6) 0.55; 7) 0.81; 8) 1; 9) 1.025; 10) 1.05; 11) 1.075 m.

TABLE 1. Comparison of the Pressure Drop ΔP and Mean Heat Conduction Coefficient $\overline{K}$ for Plates of Different Types

No.	Type of plate	$\Delta P \cdot 10^{-3}$, Pa	Deviation of ΔP from No. 1, %	$\overline{K}$, W/(m^2·K)	Deviation of $\overline{K}$ from No. 1, %
1	"Crow's -feet" S-crimps	0.23	0	2500	0
2	φ_0=60°	0.124	−46	2960	18
3	φ_0 = 45-70°	0.196	−15	2900	16
4	φ_0 = 45-75°	0.615	167	3460	36
5	φ_0 = 50-70°	0.221	-4	3250	30

increasing distance along the channel the angles of inclination of crimps toward the axis increase, the absolute value of ΔP grows, and this leads to a sharp increase in the pressure drop at the exit of the channel where the flow region is almost blocked by the crimps with inclination angles close to 75°.

The distributions of the heat transfer coefficients also behave in conformity with the pressure gradient. In case (1) α is maximal over the distributing portions where the velocity is maximum in absolute magnitude (Fig. 17). In versions (3)-(5) the heat transfer coefficient first falls at the inlet, because of the decrease in the velocity modulus, and then grows with φ_0.

To the distribution of α there also corresponds the distribution of the heat conduction coefficients K (Fig. 18). For case (1), when the distributions of κ_x, κ_y, and V are uniform, we obtain a rather uniform distribution of α and K. In cases (3)-(5), at the beginning of the flow, when the inclination angles of crimps are still insignificant,

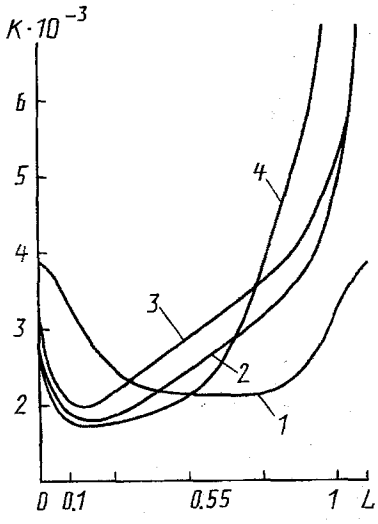

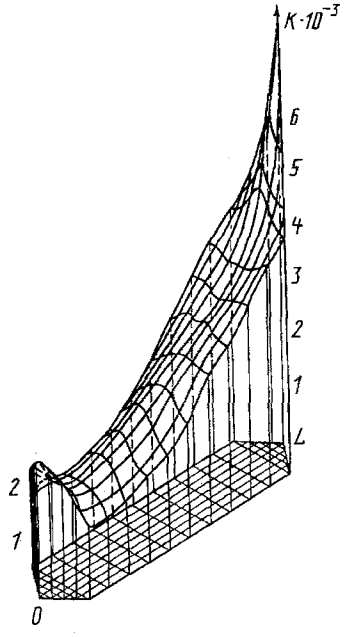

Fig. 18. Distribution of the heat conduction coefficient along the central axis of the plate: 1) for a plate of the crow's feet type; 2) for a plate with φ_0 = 45-70°; 3) for a plate with φ_0 = 50-70°; 4) for a plate with φ_0 = 45-75°.

Fig. 19. Distribution of the heat conduction coefficient over the field of a plate with S-like crimps with change in inclination angle on the central axis φ_0 from 45 to 70°.

the distribution of α and K is almost uniform (Fig. 17), although the velocity increases, but κ_y decreases, toward the periphery, and this leads to the equilization of the distribution of the heat transfer coefficient. Hereafter K grows in accord with α (Fig. 19).

From Table 1 it is seen that for plates with S-like crimps $\overline{K}$ is higher at smaller energy expenditures, except for the fourth case where the pressure drop increases sharply at the exit due to the large inclination angles of crimps. From this we can conclude that plates with S-like crimps are more efficient.

The qualitative results agree with the data of the experiments with water.

Because of the complexity of fabricating a stamped plate, we selected a smooth sheet of 0.3E-type plate and soldered on it wires in the form of straight and S-like crimps (see Fig. 12).

Comparison of the heat flux obtained on the stamped plate with that obtained on plates with soldered straight crimps showed that the former is 28% more efficient.

The experiments on plates depicted in Fig. 12 show that at identical pressure differences the mean heat conduction coefficient on a plate with S-like crimps is 30% higher than for a plate with soldered straight crimps.

NOTATION

c, heat capacity coefficient, J/(kg·K); d_{eq}, equivalent diameter, m; H, plate width, m; h, height of crimp, m; K, heat conduction coefficient, W/(m^2·K); L, length of plate, m; l, step of corrugated plate, m; M, number of divisions on computational grid along y; N, number of divisions on computational grid along x; P, pressure, Pa; Q, fluid flow rate, m^3/sec; R, radius of curvature along S-like crimp, m; V, fluid velocity, m/sec; V_0, fluid velocity at the inlet of heat exchanger channel, m/sec; x, transverse coordinate; y, longitudinal coordinate; $\mathrm{Re} = V\rho d_{eq}/\mu$, Reynolds number; $\mathrm{Re}_0 = V_0\rho d_{eq}/\mu$, Reynolds number at the inlet of channel; $\mathrm{Pr} = \mu c/\lambda_{fl}$, Prandtl number; α, heat transfer coefficient, W/(m^2·K); δ_{pl}, plate thickness, m; λ, thermal conductivity coefficient, W/(m·K); φ, angle of inclination of crimp to the central axis of the plate, deg; φ_0, angle of inclination of crimp at the inlet and outlet of

channel, deg; μ, viscosity, Pa·sec; ρ, density, kg/m^3; ξ, resistance coefficient. Indices: x, y, value of quantity along direction of respective coordinate; pl, plate; fl, fluid; 1, value for inlet-outlet section; 2, value for main field of plate.

REFERENCES

1. N. I. Buleev, The Spatial Model of Turbulent Exchange [in Russian], Moscow (1989).
2. L. M. Kovalenko and A F. Glushkov, Heat Exchangers with Heat Transfer Intensification [in Russian], Moscow (1986).
3. L. L. Tovazhnyanskii, P. A. Kapustenko, and V. A. Tsybul'nik, Énergetika, No. 9, 123-125 (1980).
4. L. L. Tovazhnyanskii and P. A. Kapustenko, Énerg. Mashinostroenie, (Khar'kov), Vyp. 34, pp. 46-50 (1982).
5. L. L. Tovazhnyanskii, Increase of the Efficiency, Improvement of the Processes and Apparatus of Chemical Industries (Abstracts of papers), Pt. 2, pp. 4-6, Khar'kov (1985).
6. R. E. Collins, Fluid Flow through Porous Materials [Russian translation], Moscow (1964).
7. L. M. Milne-Thomson, Theoretical Hydrodynamics [Russian translation], Moscow (1964).
8. E. Feder, Fractals [Russian translation], Moscow (1991).
9. L. L. Tovazhnyanskii, P. A. Kapustenko, and M. S. Chus', Increasing the Efficiency and Improving the Processes and Apparatus of Chemical Industries (Abstracts of papers), Pt. 1, pp. 96-97, L'vov (1988).
10. Plate Heat Exchanging Apparatus: Catalogue, Moscow (1983).
11. L. P. Pertsev, O. I. Gurov, V. F. Lupyr', L. M. Kovalenko, L. V. Derzhanova, L. M. Ul'ev, and V. V. Drozdov, Application for a patent No. 4860008 USSR The Packet of a Plate-type Heat Exchanger, Decision of grant of 30.07.91.
12. L. P. Pertsev, L. M. Ul'ev, and G. F. Potebnya, 8th All-Union Conf. "Two-phase Flow in Power Machines and Apparatus" (Abstracts of papers), Vol. 1, pp. 311-313, Leningrad (1990).
13. L. P. Pertsev, L. M. Ul'ev, and G. F. Potebnya, 8th All-Union. Conf. "Two-phase Flow in Power Machines and Apparatus" (Abstracts of papers), Vol. 3, pp. 133-135, pp. 133-135, Leningrad (1990).